Journal of
Materials Chemistry A

Accepted Manuscript

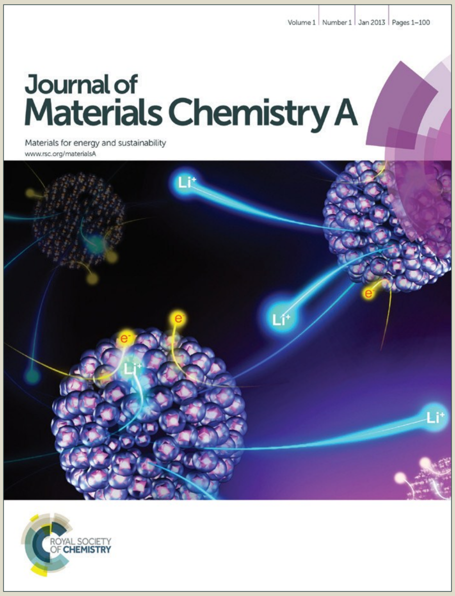

ROYAL SOCIETY
OF CHEMISTRY

www.rsc.org/materialsA

Journal of Materials Chemistry A

ARTICLE

TCO-free conducting polymers/carbon clothes as the flexible electro-catalytic counter electrodes for dye-sensitized solar cells

Received 00th January 20xx,
Accepted 00th January 20xx

DOI: 10.1039/x0xx00000x

www.rsc.org/

Chun-Ting Li,[a] Yi-Feng Lin,[b] I-Ting Chiu,[a] and Kuo-Chuan Ho[a, b,*]

Three kinds of water-soluble conducting polymers (CPs), including polypyrrole-*block*-poly(caprolactone) (PPy:PCL), poly(3,4ethylenedioxythiophene):poly(styrenesulfonate) (PEDOT:PSS), and sulfonated poly(thiophene-3-[2-(2-methoxyethoxy)ethoxy]-2,5-diyl) (s-PT), were used to decorate on the surface of fluorine-doped tin oxide (FTO) or carbon cloth (CC) separately; they were denoted as PPy:PCL/FTO, PEDOT:PSS/FTO, s-PT/FTO, PPy:PCL/CC, PEDOT:PSS/CC, and s-PT/CC and were used as the electro-catalytic counter electrodes (CEs) for dye-sensitized solar cells (DSSCs). When a DSSC coupled with a CP-coated CC as a CE, the higher solar-to-electricity conversion efficiency (η) can be obtained than that of the cell with the same CP-coated FTO as the CE. This is due to the fact that the networked carbon fibers in a CC substrate provided large surface areas, high conductivity, and directional electron transfer pathways simultaneously. Therefore, the networked carbon fibers in a CC substrate worked as the conductive cores, while the coated CPs played the important role as the electro-catalytic shell for triggering reduction of I_3^-. Among all the electrodes, the s-PT/CC renders the best η of 8.45% to its DSSC, even better than that of the cell with the traditional Pt/FTO CE, due to (1) the good intrinsic electro-catalytic ability of s-PT toward I_3^- reduction, (2) the good conductivity of s-PT in the absence of any non-conducting component (*e.g.*, the PCL in PPy:PCL or the PSS in PEDOT:PSS), (3) the large surface area and orientated electron transfer pathways provided by the CC substrate. It was concluded that the low-cost, highly efficient, and flexible s-PT/CC electrode was an attractive substitution for the expensive Pt/FTO electrode. Moreover, the extra low-weight s-PT/CC electrode was very suitable for the large-scale roll-to-roll process, which benefits the future industrialization of the DSSCs.

1. Introduction

Conducting polymers (CPs) are one of the mostly used materials in various electronics due to their excellent electrochemical properties, high electrical conductivities, good stabilities, and low-costs. Recently, the CPs were reported to have good electro-catalytic abilities toward iodide/triiodide (I^-/I_3^-) redox reaction.[1-3] Therefore, plenty of researches were focused on using CPs as effective electro-catalysts for the counter electrodes (CEs) of dye-sensitized solar cells (DSSCs) in order to replace the traditional noble metal, platinum (Pt).[4-6] Several highly efficient CPs have been proposed, including polyaniline (PANI),[7-9] polypyrrole (PPy),[10-14] poly(3,4-ethylenedioxythiophene) (PEDOT),[15-18] poly(3,4-ethylene-dioxythiophene):poly(styrenesulfonate) (PEDOT:PSS),[14,15,19] poly(3,4-propylene-dioxythiophene) (PProDOT),[17,20,21] poly(3,3-dimethyl-3,4-dihydro-2*H*-thieno(3,4-*b*)(1,4)dioxepine) (PProDOT-Me$_2$),[17] poly(3,3-diethyl-3,4-dihydro-2*H*-thieno-(3,4-*b*)(1,4)dioxepine) (PProDOT-Et$_2$),[17,20] *etc.* Extensive literature reviews revealed that the highly efficient CP-based CEs, which can render their DSSCs high solar-to-electricity conversion efficiencies (η) up to 8%, were almost prepared via an electro-polymerization process. However, electro-polymerization process has some drawbacks, including the waste of water, the difficulty in large-scale fabrication, and the complication of controlling the uniformity of the film *etc.* Therefore, the exploration of water-soluble CPs becomes more and more important due to the fact that water-soluble CPs are suitable for the large-scale roll-to-roll fabrication process with good uniformity, high conductivity, and low fabrication cost. Among all the water-soluble CPs, the most well-known water-soluble CP is PEDOT:PSS, which is the only water-soluble CP that had used as the CEs in DSSCs. A PEDOT:PSS film generally showed up a very smooth morphology, indicating its lack of sufficient electrochemical active surface.[14,15,19,22-24] So that the η of the DSSCs with PEDOT:PSS films as the CEs was restricted. Besides, PEDOT:PSS is always accompanied with the non-conducting component, PSS; thereby the conductivity and electro-catalytic ability of PEDOT:PSS are often limited.

To have a high active surface on a CE, a water soluble CP of polypyrrole-*block*-poly(caprolactone) (PPy:PCL) was firstly introduced for DSSCs in this study, because the PPy-based CPs

---

[a] *Department of Chemical Engineering, National Taiwan University, Taipei 10617, Taiwan. E–mail: kcho@ntu.edu.tw; Tel: +886–2–2366–0739; Fax: +886–2–2362–3040.*
[b] *Institute of Polymer Science and Engineering, National Taiwan University, Taipei 10617, Taiwan.*

Electronic Supplementary Information (ESI) available. See DOI: 10.1039/x0xx00000x

films were normally composed of spherical PPy nanoparticles.[10,11] To exclude the non-conducting components on a CE, another water soluble CP of sulfonated poly(thiophene-3-[2-(2-methoxyethoxy)ethoxy]-2,5-diyl) (s-PT) was also introduced in DSSCs. In this research, three different water-soluble CPs, including PPy:PCL, PEDOT:PSS, and s-PT, were used for preparing the low-cost and good electro-catalytic CEs. Since the usage of the transparent conducting oxide (TCO, *i.e.*, fluorine–doped tin oxide (FTO) or tin-doped indium oxide (ITO)) causes a high cost for the DSSCs, applying a TCO-free conducting substrate is no doubt an effective approach to reduce the fabrication cost. The cheap, low-weight, and flexible carbon clothes (CC) were proposed as the conductive substrates in this study (**Scheme 1**). The networked carbon fibers in a CC substrate worked as a conductive core, while the coated CPs played an important role of the shells in triggering the electro-catalytic reduction of I_3^-. Thus, the CC substrate not only provided large surface areas but also gave fast and directional electron transfer pathways. When coating s-PT on CC (denoted as s-PT/CC), it was surprised to find that the DSSC with s-PT/CC as a flexible CE reached the highest η of 8.45%, which is even higher than those of the cells with Pt CEs, *i.e.,* Pt/FTO (8.07%) or Pt/CC (7.08%). In brief, the electrode of s-PT/CC showed a great potential to replace the expensive Pt electrode, because it is cheap, low-weight, flexible, simple fabrication, environmental-friendly, and suitable for the large-scale roll-to-roll fabrication for future industrialization of DSSCs.

2. Experimental

2.1. Materials

Conducting polymer (CP) solutions: poly(3,4-ethylenedioxythiophene):poly(styrenesulfonate) aqueous solution (PEDOT:PSS, PH1000) was obtained from Heraeus; sulfonated-poly(thiophene-3-[2-(2-methoxyethoxy)-ethoxy]-2,5-diyl) aqueous solution (s-PT, 2% of s-PT dispersed in a mixture of 1,2-propanediol/isopropanol/water = 3/2/1 in volume ratio) and polypyrrole-*block*-poly(caprolactone) solution (PPy:PCL, 0.3-0.7 wt.% of PPy:PCL dispersed in nitromethane with *p*-toluenesulfonate as the dopant) were both obtained from Sigma Aldrich. Conductive substrates: fluorine–doped tin oxide glass (FTO, TEC–7, 7 Ω sq.$^{-1}$) was purchased from NSG America, Inc., New Jersey, USA; carbon cloth (CC, W0S1002, thickness = 0.36 mm, basic weight = 120 g cm^{-2}, sheet resistance = 0.60 Ω sq.$^{-1}$) was purchased from CeTech Co., Ltd., Taiwan.

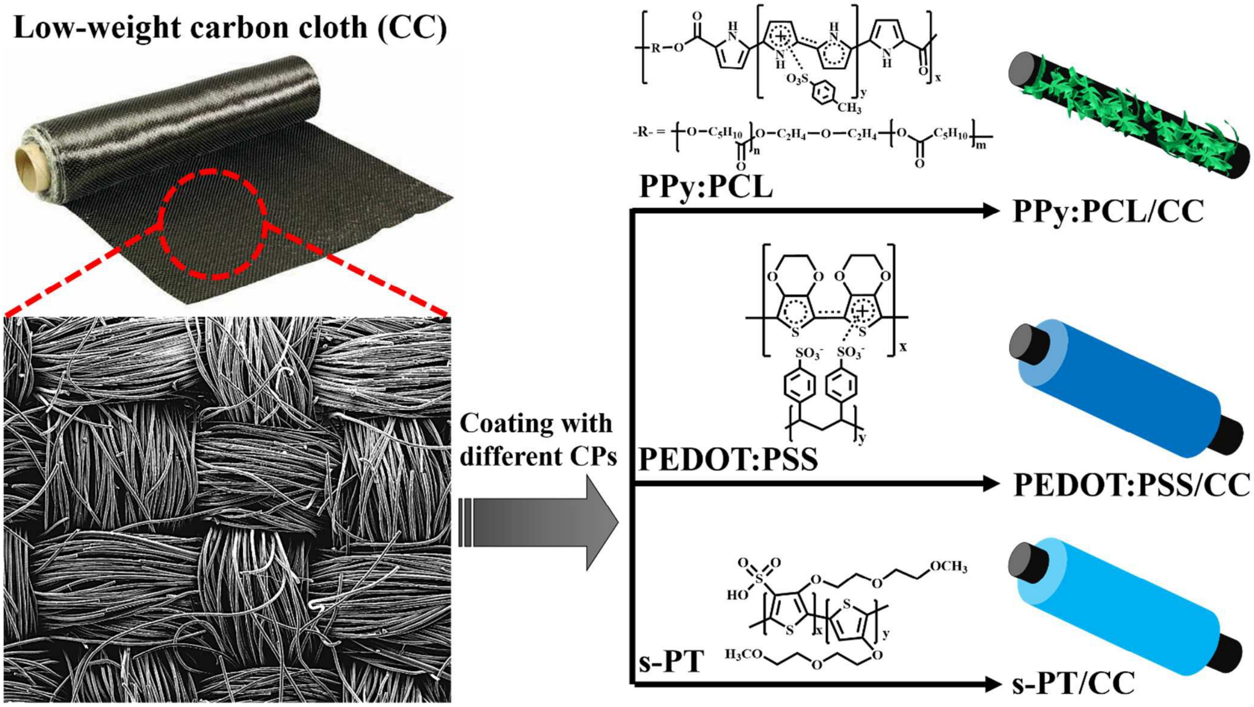

Scheme 1 The sketch of the networked carbon fibers in a carbon cloth substrate and the core-shell structures of the conducting polymers (CPs) coated carbon cloth electrodes (denoted as PPy:PCL/CC, PEDOT:PSS/CC, and s-PT/CC, separately). The molecular structures of PPy:PCL, PEDOT:PSS, and s-PT are also shown.

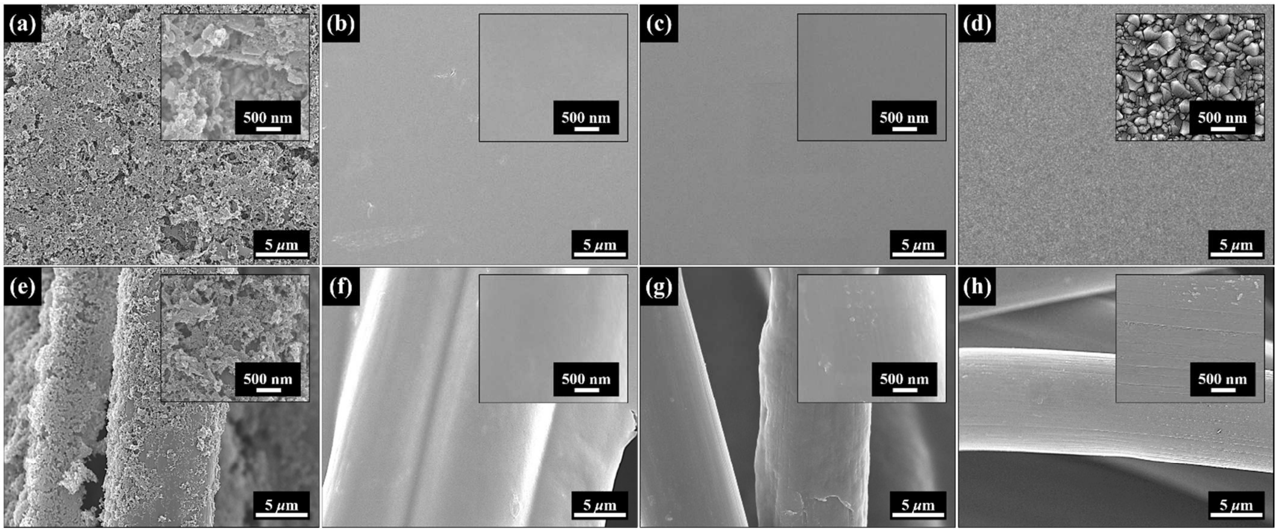

Fig. 1 FE–SEM images of the CEs of (a) PPy:PCL/FTO, (b) PEDOT:PSS/FTO, (c) s-PT/FTO, (d) Pt/FTO, (e) PPy:PCL/CC, (f) PEDOT:PSS/CC, (g) s-PT/CC, (h) Pt/CC; the insets in the figures are obtained at higher resolution.

Solvent: acetonitrile (ACN, 99.99%), nitric acid (HNO_3, *ca.* 65% solution in water), and acetone (99%) were obtained from J. T. Baker; 3-methoxypropionitrile (MPN, 99%) and *tert*–butyl alcohol (TBA, 96%) were obtained from Alfa Aesar; ethanol (EtOH, 99.5%), isopropyl alcohol (IPA, 99.5%), 2–methoxyethanol (99.9%), hydrogen peroxide (H_2O_2, *ca.* 35% solution in water), and sulfuric acid (H_2SO_4, > 95%) were obtained from Sigma Aldrich. Titanium precursors: titanium tetraisoproproxide (TTIP, >98%) was obtained from Sigma Aldrich; commercial transparent TiO_2 paste (Ti–nanoxide HT/SP, average diameter ~ 13 nm, denoted as HT/SP paste) was obtained from Solaronix, S.A., Aubonne, Switzerland; commercial light scattering TiO_2 particles (ST–41, average diameter ~ 200 nm) were obtained from Ishihara Sangyo, Ltd., Japan. Dye: cis-diisothiocyanato bis(2,2'-bipyridyl-4,4'-dicarboxylato) ruthenium (II) bis(tetrabutylammonium) (N719) was purchased from Solaronix, S.A., Aubonne, Switzerland). Redox species: lithium iodide (LiI, synthetical grade) and iodine (I_2, synthetical grade) were obtained from Merck; 1,2–dimethyl–3–propylimidazolium iodide (DMPII, >99%) was obtained from Tokyo Chemical Industry Co., Ltd., Japan. Supporting electrolytes: lithium perchlorate ($LiClO_4$, ≥98.0%) was obtained from Sigma Aldrich; guanidinium thiocyanate (GuSCN, ≥99%) and 4-*tert*-butylpyridine (TBP, 99.5%) were obtained from Acros. Other polymers: poly(ethylene glycol) (PEG, MW~20,000) was obtained from Merck; Surlyn® film (SX1170–60, thickness = 60 μm) was purchased from Solaronix, S.A., Aubonne, Switzerland.

2.2. Characterizations of the substrates and preparations of the counter electrodes

The FTO conductive glasses were firstly cleaned via the ultrasonication in the bathes of neutral cleaner, de-ionized water, acetone, and isopropanol, sequentially. Carbon clothes (CCs) were cleaned via soaking into an acid mixture of $H_2O_2/H_2SO_4=7/3$ (in volume) for 1 week. To clarify the functions of the FTO and CC substrates, three techniques were used: (1) the Brunauer–Emmett–Teller (BET) surface area measurement (ASAP2010, Micromeritics, USA), (2) a four-point probe technique to obtain the sheet resistance (related to the electrical conductivity, Keithley 2400, Keithley Instruments Inc., USA), and (3) the cyclic voltammetry (CV) analysis to determine the electro-catalytic ability of a film toward I_3^- reduction. The CV analysis was performed by a potentiostat/galvanostat (PGSTAT 30, Autolab, Eco–Chemie, Utrecht, the Netherlands) in a three-electrode system. A bare FTO or a CC substrate was used as the working electrodes (anodes) individually, while a Pt foil and a Ag/Ag^+ were used as the cathode and reference electrodes, respectively. The electrolyte for CV analysis contained 10.0 mM LiI, 1.0 mM I_2, and 0.1 M $LiClO_4$ in ACN. A scan rate of 100 mV s^{-1} was used.

Four kinds of electro-catalytic films (*i.e.*, PPy:PCL, PEDOT:PSS, s-PT, and Pt) were individually coated on both FTO and CC substrates. In the case of all conducting polymer films, the above-mentioned precursor solutions were directly used without further purification. Films of PPy:PCL, PEDOT:PSS, and s-PT were separately drop-coated on FTO substrates with a controlled area of 1 cm^2 using 200 μL of their pertinent precursors, and were dried at 120 ^oC on a hot-plate. Accordingly, the electrodes of PPy:PCL/FTO, PEDOT:PSS/FTO, and s-PT/FTO were obtained. Similarly, films of PPy:PCL, PEDOT:PSS, and s-PT were also coated on CC substrates to obtain the electrodes of PPy:PCL/CC, PEDOT:PSS/CC, and s-PT/CC, respectively. On the other hand, the Pt films were separately DC-sputtered on FTO and CC substrates to obtain the electrodes of Pt/FTO and Pt/CC, respectively, using the same fabrication process described in our previous research.[25]

2.3. DSSCs assembly

A 20 μm TiO_2 film adsorbed with N719 dye was used as a photoanode in a DSSC. The photoanode was consisted of a TiO_2 compact layer and a 20 μm porous TiO_2 film, which were prepared as follows. (1) A 100 nm TiO_2 compact layer was firstly spin-coated on a cleaned FTO substrate using a precursor solution of TTIP/2–methoxyethanol = 1/3 (in weight ratio). (2) A 20 μm porous TiO_2 film, which is composed of a 10 μm commercial transparent layer, a 5 μm home-made transparent layer, and a 5 μm home-made scattering layer, was coated on the compact layer by a doctor blade technique using a commercial transparent paste (above-mentioned HT/SP paste), a home-made transparent paste,[25] and a home-made scattering paste,[25] respectively. (3) Each TiO_2 layer was sintered at 500 ºC for 30 min in an air atmosphere. (4) The sintered TiO_2 film with an active area of 0.16 cm^2 was immersed in 5×10^{-4} M N719 dye solution at room temperature for 24 h. Thus, a dye adsorbed TiO_2 photoanode was obtained. Finally, a photoanode was assembled with a CE using a 60 μm-thick Surlyn® as the spacer. The iodide electrolyte, containing 0.1 M LiI, 1.0 M DMPII, 0.04 M I_2, and 0.5 M TBP in ACN/MPN = 8/2 (in volume ratio), was injected into the gap between these two electrodes by capillarity.

3. Results and discussion

3.1. The roles of the FTO and CC substrates

The surface areas of bare FTO and CC substrates are 84 and 1142 cm^2 g^{-1}, respectively; these values were quantified by the BET measurements. And the sheet resistances (inversely proportional to the conductivities) of bare FTO and CC substrates are 7.00 and 0.60 Ω $sq.^{-1}$, respectively, obtained by the four-point probe measurement. It can be verified that the bare CC substrate provides a larger surface area and a higher conductivity than those of the bare FTO substrate. In **Fig. S1** of the **Electronic Supplementary Information**, the CV curves of bare FTO and bare CC substrates both show no redox peaks for the I^-/I_3^- redox couple, indicating both of these substrates can't trigger the I_3^- reduction. In brief, the newly introduced CC substrate is confirmed to provide only high conductivity and large surface area, but not electro-catalytic ability toward I_3^- reduction.

3.2. Morphology

Surface morphological images of various electrodes, including PPy:PCL/FTO, PEDOT:PSS/FTO, s-PT/FTO, Pt/FTO, PPy:PCL/CC, PEDOT:PSS/CC, s-PT/CC, and Pt/CC, are obtained by field–emission scanning electron microscopy (FE–SEM, Nova NanoSEM 230, FEI, Oregon, USA), and are shown in **Fig. 1**. The electrodes of PPy:PCL/FTO and PPy:PCL/CC are both composed of irregular PPy:PCL nanoparticles to show a porous structure as shown in **Fig. 1a** and **Fig. 1e**, respectively, however, a severe aggregation of the PPy:PCL nanoparticles was also observed on both electrodes. An exposed FTO surface with a triangular pyramid-like structure was clearly shown in the inset of **Fig. 1a**, while an uncovered CC surface with a flat structure can be randomly found in **Fig. 1e**. Although all the PPy:PCL films are very porous, indicating their large surface area, the poor coverages and the fragile contacts of PPy:PCL films to both FTO and CC substrates suggest that they are unfavorable electro-catalytic films. The electrodes of PEDOT:PSS/FTO (**Fig. 1b**) and s-PT/FTO (**Fig. 1c**) both possess a very smooth and planar surface, indicating their insufficient electro-catalytic surface areas and lacks of orientated electron transfer pathways, causing the poor electro-catalytic ability. The electrodes of PEDOT:PSS/CC (**Fig. 1f**) and s-PT/CC (**Fig. 1g**) are both composed of the networked carbon fibers that are well-covered with their CPs. Thus, a core-shell like structure using the networked carbon fibers as the conductive cores and the decorated CPs as electro-catalytic shells can be observed. Although each carbon fiber on the PEDOT:PSS/CC and s-PT/CC electrodes shows a smooth morphology, those electrodes still possess both large surface areas and directional electron transfer pathways provided by the CC substrate. The electrodes of Pt/FTO and Pt/CC are both composed of Pt nanoparticles on the substrates, as shown in **Fig. 1d** and **Fig. 1h**, respectively. In **Fig. 1d**, a flat, uniform, and compact Pt film was obtained on an FTO. However, a discontinued Pt film was observed on a CC as shown in **Fig. 1h**, indicating a poor electro-catalytic surface.

3.3. Photovoltaic performance

Photovoltaic parameters of the DSSCs with various CEs were calculated by the pertinent photocurrent density–voltage curves (*J*–*V* curves) measured by a potentiostat/galvanostat (PGSTAT 30, Autolab, Eco–Chemie, Utrecht, the Netherlands) at AM 1.5G sun light illumination, using a class A quality solar simulator (XES–301S, AM1.5G, San–Ei Electric Co., Ltd., Osaka, Japan). The incident light intensity of 100 mW cm^{-2} was calibrated with a standard Si cell (PECSI01, Peccell Technologies, Inc., Kanagawa, Japan). The *J*–*V* curves for the cells with the CEs coated on the FTO substrates, including PPy:PCL/FTO, PEDOT:PSS/FTO, s-PT/FTO, and Pt/FTO are shown in **Fig. 2a**, and the corresponding photovoltaic parameters are summarized in **Table 1**. The DSSCs with CEs of PPy:PCL/FTO, PEDOT:PSS/FTO, and s-PT/FTO show the poor cell efficiencies (η's) of 3.86%, 4.74%, and 5.40%, respectively. Since the electro-catalytic reduction of triiodide ions (I_3^-) on the surface of a CE is a rate-determining step in a DSSC, the slow consumption of I_3^- causes the severe energy loss and thus the poor cell efficiency.[1,6,26] With insufficient electro-catalytic surface areas on the CEs of CPs/FTO (*i.e.*, PPy:PCL/FTO, PEDOT:PSS/FTO, and s-PT/FTO), their DSSCs have the limited and the poor performances. Among these three cells, the CE of PPy:PCL/FTO has the most porous morphology, however, its DSSC has the lowest η due to the very weak adhesion between PPy:PCL nanoparticles and the FTO substrate. In the case of the cell with Pt/FTO, a good η of 8.07% with an open–circuit voltage (V_{oc}) of 0.71 V, a short-circuit current (J_{sc}) of 15.71 mA cm^{-2}, and a fill factor (*FF*) of 0.72 is obtained due to the outstanding electro-catalytic ability of Pt.[27,28]

The *J–V* curves for the cells with the CEs on the CC substrates, including PPy:PCL/CC, PEDOT:PSS/CC, s-PT/CC, and Pt/CC are shown in **Fig. 2b**, and the corresponding photovoltaic parameters are also summarized in **Table 1**. The DSSCs with CEs of PPy:PCL/CC, PEDOT:PSS/CC, and s-PT/CC show the η's of 6.78%, 7.60%, and 8.45%, respectively. It is noticed that a cell with a CP coated on CC shows about 1.5 times higher η than that of the cell with the same CP coated on FTO; because the networked carbon fibers in a CC substrate provided large surface areas, high conductivity, and directional electron transfer pathways simultaneously. In the case of the cell with a Pt/CC as a CE, a decreased η of 7.08% is obtained, compared to that of the cell with Pt/FTO; this is owing to the lesser electro-catalytic ability of Pt/CC given by the discontinued Pt film covered on its CC substrate. Among these four cells with the CEs based on the CC substrates, the s-PT/CC renders the best η of 8.45% to its DSSC with a V_{oc} of 0.71 V, a J_{sc} of 15.90 mA cm^{-2}, and a *FF* of 0.75 due to (1) the good intrinsic electro-catalytic ability of s-PT toward I_3^- reduction, (2) the good conductivity of s-PT in the absence of any non-conducting component (*e.g.*, the PCL in PPy:PCL or the PSS in PEDOT:PSS), (3) the large surface area and orientated electron transfer pathways provided by the CC substrate.

Incident photon–to–current conversion efficiency (IPCE) of a DSSC was measured at the short-circuit condition and recorded by the above-mentioned potentiostat/galvanostat under a monochromatic light illumination in a wavelength range of 400-800 nm. To obtain the IPCE data, another class-A solar simulator (PEC–L11, AM1.5G, Peccell Technologies, Inc., Kanagawa, Japan) equipped with a monochromator (model 74100, Oriel Instrument, California, USA) was used. The incident radiation flux (φ) was obtained by using an optical detector (model 818-SL, Newport, California, USA) and a power meter (model 1916-R, Newport, California, USA). In **Fig. 3**, the DSSCs with the CEs of PPy:PCL/CC, PEDOT:PSS/CC, s-PT/CC, and Pt/FTO give good IPCE values around 60~90% from 400 to 600 nm, confirming their good DSSCs' performance.

Table 1 Photovoltaic parameters of the DSSCs with various CEs, measured at 100 mW cm^{-2} (AM 1.5G) light intensity.

CEs	η (%)	V_{oc} (V)	J_{sc} (mA cm^{-2})	FF
PPy:PCL/FTO	3.86	0.66	12.58	0.46
PEDOT:PSS/FTO	4.74	0.67	12.81	0.55
s-PT/FTO	5.40	0.68	13.26	0.60
Pt/FTO	8.07	0.71	15.71	0.72
PPy:PCL/CC	6.78	0.70	14.52	0.67
PEDOT:PSS/CC	7.60	0.70	14.95	0.72
s-PT/CC	8.45	0.71	15.90	0.75
Pt/CC	7.08	0.71	14.86	0.67

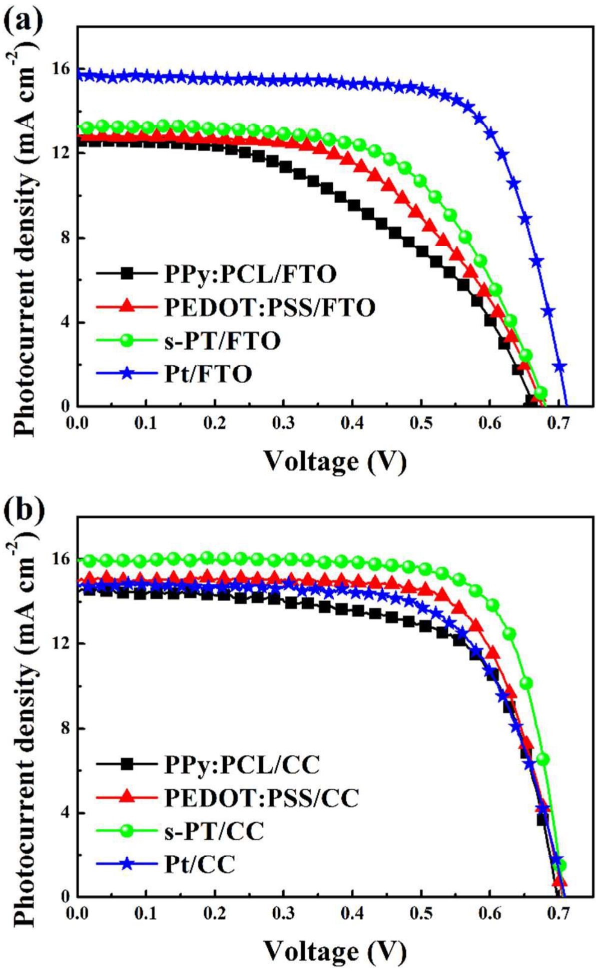

Fig. 2 Photocurrent density–voltage curves of the DSSCs with the CEs of (a) PPy:PCL/FTO, PEDOT:PSS/FTO, s-PT/FTO, Pt/FTO, and (b) PPy:PCL/CC, PEDOT:PSS/CC, s-PT/CC, Pt/CC, measured at 100 mW cm^{-2} (AM 1.5G) light intensity.

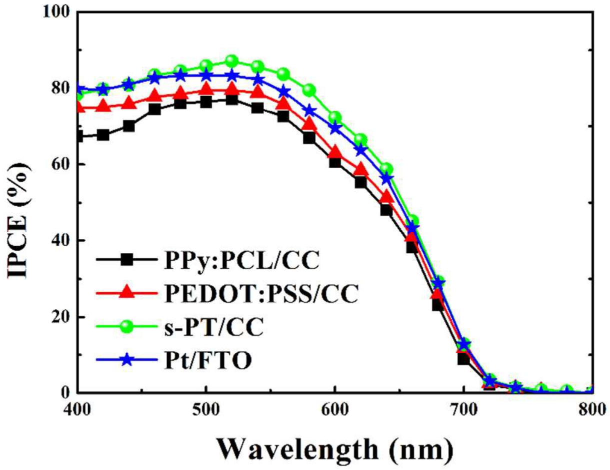

Fig. 3 Incident photon–to–current conversion efficiency (IPCE) curves of the DSSCs with the CEs of PPy:PCL/CC, PEDOT:PSS/CC, s-PT/CC, and Pt/FTO.

Besides, each IPCE curve is used to further integrated to get a short-circuit current density ($J_{sc\text{-}IPCE}$) value. The $J_{sc\text{-}IPCE}$ values for the cells with PPy:PCL/CC, PEDOT:PSS/CC, s-PT/CC, and Pt/FTO are 11.54, 12.21, 13.45, and 13.01 mA cm^{-2}, respectively, which agree well with the J_{sc} values obtained from the J–V curves. It is notable that the best IPCE value (87% at 520 nm) and the highest $J_{sc\text{-}IPCE}$ value (13.45 mA cm^{-2}) are obtained for the DSSC with an s-PT/CC CE; these values are even higher than those of the DSSC with a Pt/FTO CE.

3.4. Cyclic voltammetry

To further quantify the electro-catalytic ability of a CE, cyclic voltammetry (CV) technique was applied to investigate the reduction of I_3^- at the CE/electrolyte interface.[6,29,30] CV was performed in a three-electrode electrochemical system and recorded by the above-mentioned potentiostat/galvanostat. The electrodes of PPy:PCL/CC, PEDOT:PSS/CC, s-PT/CC, and Pt/FTO were used as the working electrodes (anode) individually, while a Pt foil and a Ag/Ag$^+$ were used as the cathode and reference electrodes, respectively. The electrolyte for CV analysis contained 10.0 mM LiI, 1.0 mM I_2, and 0.1 M $LiClO_4$ in ACN. A scan rate of 100 mV s^{-1} was used. In **Fig. 4**, the cathodic peak current density (J_{pc}) of a CV curve indicates the overall electro-catalytic ability of an electrode for I_3^- reduction (**Eqn. (1)**), and the larger value of J_{pc} reflects the better overall electro-catalytic ability.

$$I_3^- + 2e^- \rightarrow 3I^- \qquad (1)$$

The J_{pc} values of PPy:PCL/CC, PEDOT:PSS/CC, s-PT/CC, and Pt/FTO are 0.67, 0.84, 1.32, and 1.19 mA cm^{-2}, respectively (**Table 2**). Among all the CPs/CC electrodes, the J_{pc} values show their electro-catalytic ability of the electrodes in a tendency of s-PT/CC > PEDOT:PSS/CC > PPy:PCL/CC, which agrees with the tendencies of the J_{sc}, FF, and thereby the η values of the pertinent DSSCs. Comparing to the electrodes of PEDOT:PSS/CC and PPy:PCL/CC, the s-PT/CC possesses the best electro-catalytic ability due to the absence of any non-conducting component in s-PT and the good adhesion of s-PT film to CC. Moreover, the s-PT/CC even reaches better electro-catalytic ability than that of Pt/FTO due to the larger electro-catalytic surface areas and the fast, orientated, and multiple electron transfer pathways provided by CC substrate. It is concluded that the electrode of s-PT/CC has an outstanding electro-catalytic ability toward I_3^- reduction, even better than that of Pt.

3.5. Tafel polarization plot

To explore the practical electro-catalytic ability of a CE in a DSSC, Tafel polarization technique is applied in an electrolyte used in the J-V curve measurement; the electrolyte is composed of 0.1 M LiI, 1.0 M DMPII, 0.04 M I_2, and 0.5 M TBP in ACN/MPN = 8/2 (in volume ratio). Comparing to the CV analysis, the electrolyte used for Tafel analysis contains much higher concentration of iodides.

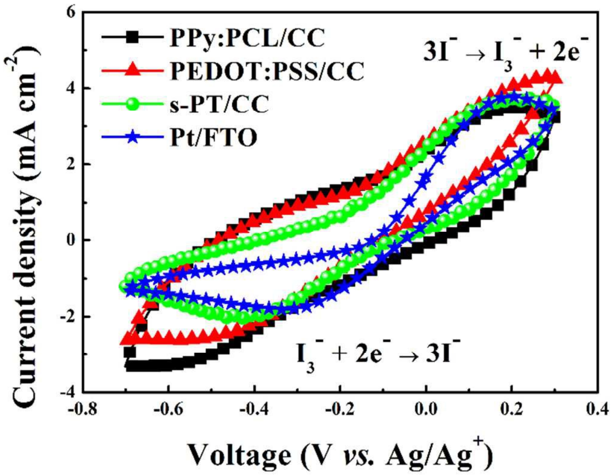

Fig. 4 Cyclic voltammograms of various CEs, measured at a scan rate of 100 mV s^{-1}.

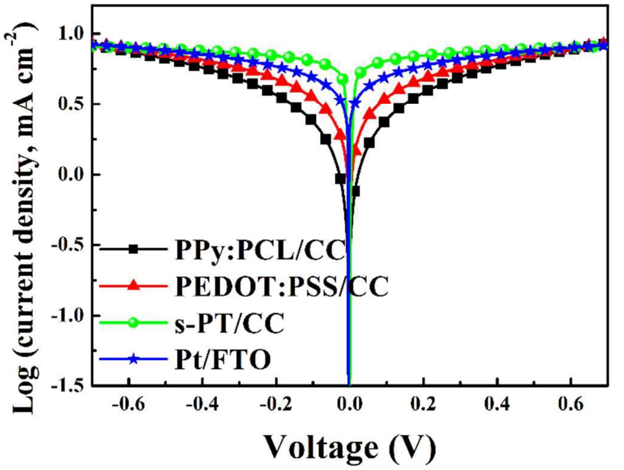

Fig. 5 Tafel polarization plot of various electro-catalytic films, measured at a scan rate of 50 mV s^{-1}.

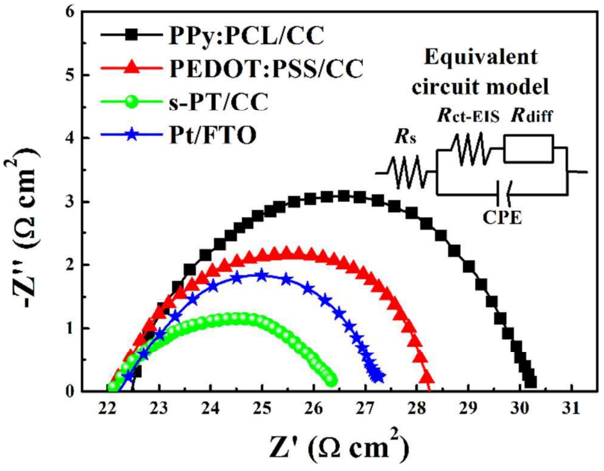

Fig. 6 Electrochemical impedance spectra of various electro-catalytic films.

Table 2 Electrochemical parameters of various electrodes.

Electrodes	J_{pc} (mA cm^{-2})	J_0 (mA cm^{-2})	$R_{ct\text{-Tafel}}$ (Ω cm^2)	$R_{ct\text{-EIS}}$ (Ω cm^2)
PPy:PCL/CC	0.67	2.63	4.88	3.91
PEDOT:PSS/CC	0.84	3.78	3.39	3.05
s-PT/CC	1.32	6.31	2.04	2.17
Pt/FTO	1.19	4.79	2.68	2.52

Based on a symmetric cell composed of the same electrode as both anode and cathode, a linear sweep voltammetry (LSV) curve is obtained at a low scan rate of 50 mV s^{-1} using the above-mentioned potentiostat/galvanostat. Accordingly, a LSV curve is converted to a logarithmic current density–voltage (*Log J–V*) curve, which gives a Tafel polarization plot.[31] A Tafel curve can be simply divided into three zones: (1) a polarization zone (|V| < 120 mV), (2) a Tafel zone (120 mV< |V| < 400 mV), and (3) a diffusion zone (|V| > 400 mV).[31]

The Tafel polarization curves of the electrodes of PPy:PCL/CC, PEDOT:PSS/CC, s-PT/CC, and Pt/FTO are shown in **Fig. 5**. The exchange current density (J_0) for a Tafel curve is obtained by extrapolating the anodic and cathodic curves in its Tafel zone and reading the cross point at 0 V. The higher value of J_0 reflects the better electro-catalytic ability of an electrode. As summarized in **Table 2**, the J_0 values of PPy:PCL/CC, PEDOT:PSS/CC, s-PT/CC, and Pt/FTO are 2.63, 3.78, 6.31, and 4.79 mA cm^{-2}, respectively, which are in a good consistency with the J_{pc} values obtained from CV analysis. Therefore, the electro-catalytic ability of an electrode is thus validated not only by CV (with lower I^-/I_3^- concentration) but also by Tafel analysis (with higher I^-/I_3^- concentration). Since the electrode of s-PT/CC shows the largest slope in its polarization zone and gives the highest J_0 values in its Tafel zone, there is no doubt that the s-PT/CC electrode possesses the best electro-catalytic ability and the fastest I_3^- reduction rate than the others, even better than the traditional Pt/FTO electrode.

On the other hand, the J_0 value of an electrode can be used to calculate the charge transfer resistance ($R_{ct\text{-Tafel}}$) at the CE/electrolyte interface in a DSSC, via **Eqn. (2)**.[31]

$$J_0 = \frac{RT}{nFR_{ct\text{-Tafel}}} \tag{3}$$

where R is the ideal gas constant, T is the absolute temperature, n is the number of electrons transferred for I_3^- reduction, and F is Faraday constant. The smaller $R_{ct\text{-Tafel}}$ value, the more amounts of electrons transferring through the CE/electrolyte interface, the faster electron transfer capability of an electrode. As summarized in **Table 2**, the $R_{ct\text{-Tafel}}$ values of PPy:PCL/CC, PEDOT:PSS/CC, s-PT/CC, and Pt/FTO are 4.88, 3.39, 2.04, and 2.68 mA cm^{-2}, respectively. It is notable that the electrode of s-PT/CC has the lowest $R_{ct\text{-Tafel}}$ value of 2.04 Ω cm^2, indicating its best electron transferring capability to render its DSSC the highest J_{sc}, FF, and thus the best η.

3.6. Electrochemical impedance spectroscopy

Electrochemical impedance spectroscopy (EIS) is further used for the precise examination of the interfacial resistances in a symmetric cell. Under an open-circuit condition, an EIS spectrum was measured between 10 mHz to 65 kHz in an AC amplitude of ±10 mV using the above-mentioned potentiostat/galvanostat equipped with an FRA2 module. Generally, an EIS spectrum for a symmetric cell has two semicircles; the first semicircle in the higher frequency region reflects the charge transfer resistance ($R_{ct\text{-EIS}}$) at the CE/electrolyte interface, while the second semicircle in the lower frequency region shows the Warburg diffusion resistance of the iodide electrolyte in the bulk solution.[6,30,32] Since the iodide electrolyte is composed of an ACN-based solvent with extremely low viscosity and good ionic conductivity, the second semicircle for the Warburg diffusion resistance is merged with the first semicircle of an EIS plot.[33,34] Thus, the EIS plots in **Fig. 6** all consist of one clear first semicircle and one ambiguous second semicircle. In accordance with the equivalent circuit shown in the inset of **Fig. 6**, the onset point of the first semicircle is the series resistance (R_s); the lower R_s, the better ohmic contact between the substrate and the coated electro-catalytic film.[35,36] The R_s values of the electrodes of PPy:PCL/CC, PEDOT:PSS/CC, s-PT/CC, and Pt/FTO are all similar, implying that the electro-catalytic films of PPy:PCL, PEDOT:PSS, s-PT, and Pt all have good adhesion to their substrates. Moreover, the $R_{ct\text{-EIS}}$ values are obtained via the fitting model based on the equivalent circuit shown in the inset of **Fig. 6**. As summarized in **Table 2**, the $R_{ct\text{-EIS}}$ values of the electrodes show a tendency of s-PT/CC < Pt/FTO < PEDOT:PSS/CC < PPy:PCL/CC, which is highly consistent with the tendency of $R_{ct\text{-Tafel}}$ values obtained from the Tafel polarization curves. It is notable that all the R_{ct} values ($R_{ct\text{-Tafel}}$ or $R_{ct\text{-EIS}}$), irrespective of their measurement techniques, show a perfect consistent with the results of J_{pc} and J_0 values. In brief, according to CV, Tafel, and EIS analyses, the electro-catalytic abilities of the electrodes follow the order of s-PT/CC > Pt/FTO > PEDOT:PSS/CC > PPy:PCL/CC. Among all the electrodes, s-PT/CC exhibits the best electro-catalytic ability for I_3^- reduction, and shows a promising potential to replace Pt.

4. Conclusions

Electrodes of PPy:PCL/FTO, PEDOT:PSS/FTO, s-PT/FTO, Pt/FTO, PPy:PCL/CC, PEDOT:PSS/CC, s-PT/CC, and Pt/CC were successfully prepared as the electro-catalytic CE for DSSCs; especially for PPy:PCL and s-PT, they are introduced in the DSSC field for the first time. When a conducting polymer film (PPy:PCL, PEDOT:PSS, or s-PT) was coated on a CC substrate, the pertinent CE renders ~1.5 times higher DSSC efficiency than that of the cell with a CE based on an FTO substrate. Since networked carbon fibers in a CC substrate worked as the conductive cores and simultaneously provided large surface areas and directional electron transfer pathways, a core-shell structure for the electrodes of conducting polymers/CC can be observed in the FE-SEM images. Thus, the conducting polymers functions as the electro-catalytic shells to trigger the I_3^- reduction. From CV and Tafel analyses, the electro-catalytic ability of an electrode was quantified by the J_{pc} and J_0, respectively; it shows a tendency of s-PT/CC > PEDOT:PSS/CC > PPy:PCL/CC. The s-PT/CC has the best electro-catalytic ability due to (1) the good intrinsic electro-catalytic ability of s-PT toward I_3^- reduction and (2) the good conductivity of s-PT in the absence of any non-conducting component (*e.g.*, the PCL in PPy:PCL or the PSS in PEDOT:PSS). From Tafel and EIS analyses, the charge transfer capability is explored using the charge transfer resistances ($R_{ct\text{-}Tafel}$ and $R_{ct\text{-}EIS}$). The s-PT/CC possesses the best charge transfer capability, even better than that of the traditional Pt/FTO; it is contributed by the large surface area and orientated electron transfer pathways provided by the CC substrate. In conclusion, the s-PT/CC electrode can be considered as a promising electro-catalytic material to replace the expensive Pt/FTO CE for DSSCs. Most of all, s-PT/CC has lots of advantages; for example, it is earth abundant, TCO-free, low-cost, highly efficient, extra low-weight, environmental friendly, flexible, and suitable for the large-scale roll-to-roll process. Therefore, s-PT/CC has an outstanding potential to utilize in future industrialized DSSCs.

Acknowledgements

This work was supported by the Ministry of Science and Technology (MOST) of Taiwan, under grant number of NSC 102-2221-E-002-186-MY3 and 103-2119-M-007-012.

Notes and references

1. Q. Tai and X. Z. Zhao, *J. Mater. Chem. A*, 2014, **2**, 13207-13218.
2. J. Theerthagiri, A. R. Senthil, J. Madhavan and T. Maiyalagan, *ChemElectroChem*, 2015, **2**, 928-945.
3. K. Saranya, M. Rameez and A. Subramania, *Eur. Polym. J.*, 2015, **66**, 207-227.
4. M. Chen, L. L. Shao, X. Qian, T. Z. Ren and Z. Y. Yuan, *J. Mater. Chem. C*, 2014, **2**, 10312-10321.
5. D. J. Yun, Y. J. Jeong, H. Ra, J. M. Kim, T. K. An, M. Seol, J. Jang, C. E. Park, S. W. Rhee and D. S. Chung, *J. Mater. Chem. C*, 2015, **3**, 7325-7335.
6. S. Yun, A. Hagfeldt and T. Ma, *Adv. Mater.*, 2014, **26**, 6210-6237.
7. Q. Li, J. Wu, Q. Tang, Z. Lan, P. Li, J. Lin and L. Fan, *Electrochem. Commun.*, 2008, **10**, 1299-1302.
8. J. Wu, Y. Li, Q. Tang, G. Yue, J. Lin, M. Huang and L. Meng, *Sci. Rep.*, 2014, **4**, 4028(1)-(7).
9. H. Wang, Q. Feng, F. Gong, Y. Li, G. Zhou and Z. S. Wang, *J. Mater. Chem. A*, 2013, **1**, 97-104.
10. J. Wu, Q. Li, L. Fan, Z. Lan, P. Li, J. Lin and S. Hao, *J. Power Sources*, 2008, **181**, 172-176.
11. S. S. Jeon, C. Kim, J. Ko and S. S. Im, *J. Mater. Chem.*, 2011, **21**, 8146-8151.
12. F. Gong, X. Xu, G. Zhou and Z. S. Wang, *Phys. Chem. Chem. Phys.*, 2013, **15**, 546-552.
13. B. He, Q. Tang, J. Luo, Q. Li, X. Chen and H. Cai, *J. Power Sources*, 2014, **256**, 170-177.
14. G. Yue, J. Wu, Y. Xiao, J. Lin, M. Huang and Z. Lan, *J. Phys. Chem. C*, 2012, **116**, 18057-18063.
15. T. L. Zhang, H. Y. Chen, C. Y. Su and D. B. Kuang, *J. Mater. Chem. A*, 2013, **1**, 1724-1730.
16. T. H. Lee, K. Do, Y. W. Lee, S. S. Jeon, C. Kim, J. Ko and S. S. Im, *J. Mater. Chem.*, 2012, **22**, 21624-21629.
17. S. Ahmad, T. Bessho, F. Kessler, E. Baranoff, J. Frey, C. Yi, M. Grätzel and M. K. Nazeeruddin, *Phys. Chem. Chem. Phys.*, 2012, **14**, 10631-10639.
18. C. T. Li, C. P. Lee, M. S. Fan, P. Y. Chen, R. Vittal and K. C. Ho, *Nano Energy*, 2014, **9**, 1-14.
19. G. Guan, Z. Yang, L. Qiu, X. Sun, Z. Zhang, J. Ren and H. Peng, *J. Mater. Chem. A*, 2013, **1**, 13268-13273.
20. K. M. Lee, P. Y. Chen, C. Y. Hsu, J. H. Huang, W. H. Ho, H. C. Chen and K. C. Ho, *J. Power Sources*, 2009, **188**, 313-318.
21. S. Ahmad, J. H. Yum, H. J. Butt, M. K. Nazeeruddin and M. Grätzel, *ChemPhysChem*, 2010, **11**, 2814-2819.
22. C. H. Chiang and C. G. Wu, *Org. Electron.*, 2013, **14**, 1769-1776.
23. D. J. Yun, J. Kim, J. Chung, S. Park, W. Baek, Y. Kim, S. Kim, Y. N. Kwon, J. Chung, Y. Kyoung, K. H. Kim and S. Heo, *J. Power Sources*, 2014, **268**, 25-36.
24. H. Wang, W. Wei and Y. H. Hu, *J. Mater. Chem. A*, 2013, **1**, 6622-6628.
25. C. T. Li, C. P. Lee, Y. Y. Li, M. H. Yeh and K. C. Ho, *J. Mater. Chem. A*, 2013, **1**, 14888-14896.
26. A. Listorti, B. O'Regan and J. R. Durrant, *Chem. Mater.*, 2011, **23**, 3381-3399.
27. Z. Zheng, J. Chen, Y. Hu, W. Wu, J. Hua and H. Tian, *J. Mater. Chem. C*, 2014, **2**, 8497-8500.
28. L. Y. Chang, C. P. Lee, R. Vittal, J. J. Lin and K. C. Ho, *J. Mater. Chem.*, 2012, **22**, 12305-12312.
29. T. N. Murakami and M. Grätzel, *Inorg. Chim. Acta*, 2008, **361**, 572-580.
30. M. Wu and T. Ma, *ChemSusChem*, 2012, **5**, 1343-1357.
31. A. Bard and L. Faulkner, *Electrochemical Methods: Fundamentals and Applications*, John Wiley & Sons, Inc., New York, 2nd Edn., 2001.
32. M. Wu, X. Lin, Y. Wang, L. Wang, W. Guo, D. Qi, X. Peng, A. Hagfeldt, M. Grätzel and T. Ma, *J. Am. Chem. Soc.*, 2012, **134**, 3419-3428.
33. L. Y. Chang, C. T. Li, Y. Y. Li, C. P. Lee, M. H. Yeh, K. C. Ho and J. J. Lin, *Electrochim. Acta*, 2015, **155**, 263-271.
34. L. Y. Chang, C. P. Lee, R. Vittal, J. J. Lin and K. C. Ho, *J. Mater. Chem. A*, 2013, **1**, 3055-3060.
35. Qing Wang, Seigo Ito, Michael Grätzel, Francisco Fabregat-Santiago, Iván Mora-Seró, Juan Bisquert, Takeru Bessho and H. Imai, *J. Phys. Chem. B*, 2006, **110**, 25210-25221.
36. P. Poudel and Q. Qiao, *Nano Energy*, 2014, **4**, 157-175.

Graphical Abstract

TCO-free conducting polymers/carbon clothes as the flexible electro-catalytic counter electrodes for dye-sensitized solar cells

Chun-Ting Li,[a] Yi-Feng Lin,[b] I-Ting Chiu,[a] and Kuo-Chuan Ho[a, b,*]

[a]*Department of Chemical Engineering, National Taiwan University, Taipei 10617, Taiwan;*
[b]*Institute of Polymer Science and Engineering, National Taiwan University, Taipei 10617, Taiwan*

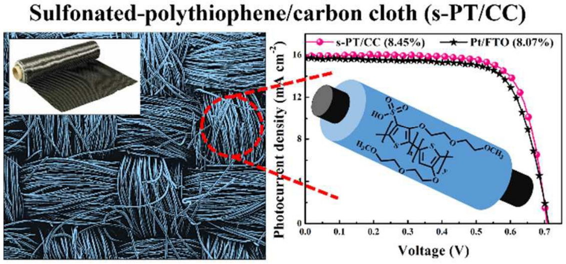
Sulfonated-polythiophene/carbon cloth (s-PT/CC)

A TCO-free counter electrode of sulfonated-polythiophene/carbon cloth gave a good cell efficiency (η) of 8.45% to its dye-sensitized solar cell, indicating its attractive potential to replace the expensive Pt/FTO (η=8.07%).